The EMBO Journal Vol.16 No.9 pp.2294–2306, 1997

Adenovirus type 5 fiber knob binds to MHC class I α2 domain at the surface of human epithelial and B lymphoblastoid cells

Saw See Hong, Lucie Karayan, Jeannette Tournier, David T.Curiel[1] and Pierre A.Boulanger[2]

Laboratoire de Virologie et Pathogénèse Moléculaires (CNRS URA 1487), Institut de Biologie, Faculté de Médecine, 34060 Montpellier, France and [1]Gene Therapy Program, Comprehensive Cancer Center, University of Alabama, Birmingham, AL 35294, USA

[2]Corresponding author
e-mail: pboulang@infobiogen.fr

Adenovirus serotype 5 (Ad5) fiber receptor was investigated using reverse antibody biopanning of a phage-displayed hexapeptide library, and virus-neutralizing monoclonal antibodies (mAbs 1D6.3 and 7A2.7) raised against recombinant Ad5 fiber knob. Both mAbs inhibited attachment of Ad5 to HeLa cells. Mimotopes of 1D6.3 showed homology with the C-terminal segment of the α2 domain of the heavy chain of human MHC class I molecules (MHC-I α2), and mimotopes of 7A2.7 were consensus to human fibronectin type III (FNIII) modules. *In vitro*, GST-fused MHC-I α2- and FNIII-derived oligopeptides interacted with recombinant fibers in a subgroup-specific manner. *In vivo*, the MHC-I α2 synthetic icosapeptide RAIVGFRVQWLRRYFVNGSR showed a net neutralization effect on Ad5 in HeLa cells, whereas the FNIII icosapeptide RHILWTPANTPAMGYLARVS significantly increased Ad5 binding to HeLa cells. Daudi cells, which lack surface expression of HLA class I molecules, showed a weak capacity for Ad5 binding. In β2-microglobulin-transfected Daudi cells, Ad5 attachment and permissivity were restored to HeLa cell levels, with 4000 receptors per cell and a binding constant of 1.4×10^{10}/M. The results suggested that the conserved region of MHC-I α2-domain including Trp167 represents a high affinity receptor for Ad5 fiber knob, whereas ubiquitous FNIII modules would serve as auxiliary receptors.

Keywords: adenovirus serotype 5/fiber knob/fiber receptor/fibronectin type III module/MHC class I heavy chain α2 domain

Introduction

The apical projection of the capsid of human adenoviruses, the fiber, is a highly asymmetrical molecule visible under the electron microscope. Its sequence, of ~580 amino acids in subgroup C adenoviruses, e.g. serotypes 2 or 5 (Ad2, Ad5), consists of three structural domains: (i) the N-terminal tail (amino acids 1–46 in Ad2), which interacts with the penton base, (ii) the shaft (amino acids 47–400) constituted of repeat motifs, and (iii) the spherical knob (or head), which contains the C-terminus and interacts with the host cell surface receptors (reviewed in Chroboczek *et al.*, 1995). The knob domains of Ad5, Ad2 and Ad3 fibers (including the shaft–knob junction) have been cloned and expressed in bacteria, insect and human cells, and all were found to occur as trimers. This confirms that signals essential for fiber trimerization are localized at the C-terminal extremity of the fiber protein as well as in the last shaft repeat (Novelli and Boulanger, 1991a,b; Hong and Engler, 1996). The isolated fiber knob retained its full cell-binding capability (Henry *et al.*, 1994; Louis *et al.*, 1994; Stevenson *et al.*, 1995).

It is generally accepted that the entry of Ad into susceptible cells is a stepwise process, consisting of (i) an initial attachment of the virion to the cell surface via the fiber, followed by (ii) a phase of endocytosis, implicating membrane components such as $\alpha_V\beta_3$ and $\alpha_V\beta_5$ integrins and the five conserved RGD motifs of the penton base (Varga *et al.*, 1991; Bai *et al.*, 1993, 1994; Belin and Boulanger, 1993; Greber *et al.*, 1993; Wickham *et al.*, 1993, 1994; Cuzange *et al.*, 1994; Mathias *et al.*, 1994; Nemerow *et al.*, 1994; Sprengel *et al.*, 1994; Goldman and Wilson, 1995; Greber and Kasamatsu, 1996). The two events can be experimentally dissociated, taking advantage of the observation that at low temperature (0–4°C) only virus–cell attachment occurs, whereas endocytosis requires 37°C (Philipson *et al.*, 1968; Lonberg-Holm and Philipson, 1969; Svensson and Persson, 1984; Svensson, 1985; Wohlfart, 1988; Defer *et al.*, 1990). In the two-step model, the fiber distal knob is considered as the domain which is responsible for the primary event of binding of the virions to the host cell plasma membrane receptor(s). Experimental data suggest that at least two distinct families of fiber receptors are involved in Ad–cell recognition, one specific for the subgroup C members (Ad2 and Ad5), and another one for the subgroup B (Ad3 and Ad7; Defer *et al.*, 1990; Stevenson *et al.*, 1995). The total number of cell binding sites for Ad2 has been estimated to range between 5×10^3 and 10×10^3 at the surface of HeLa cells (Persson *et al.*, 1985; Defer *et al.*, 1990), consisting of two types of receptors with high and low affinity, respectively (Persson *et al.*, 1985; Seth *et al.*, 1994).

The goal of the present study was to identify the cell-binding domain of the Ad5 fiber knob, and the complementary peptide motifs of host cell surface proteins which recognize the fiber knob during the event of virion attachment. To this aim, we used a novel approach, based on a method of reverse antibody biopanning of a filamentous phage-displayed random hexapeptide library, with two virus-neutralizing monoclonal antibodies (mAbs 7A2.7 and 1D6.3) raised against the recombinant Ad5 fiber knob. Their epitopes were localized to two contiguous discrete regions, one of which (1D6.3) belonged to the domain of the knob structure which has been postulated to face the cell receptor (R-sheets; Xia *et al.*, 1994). As

© Oxford University Press

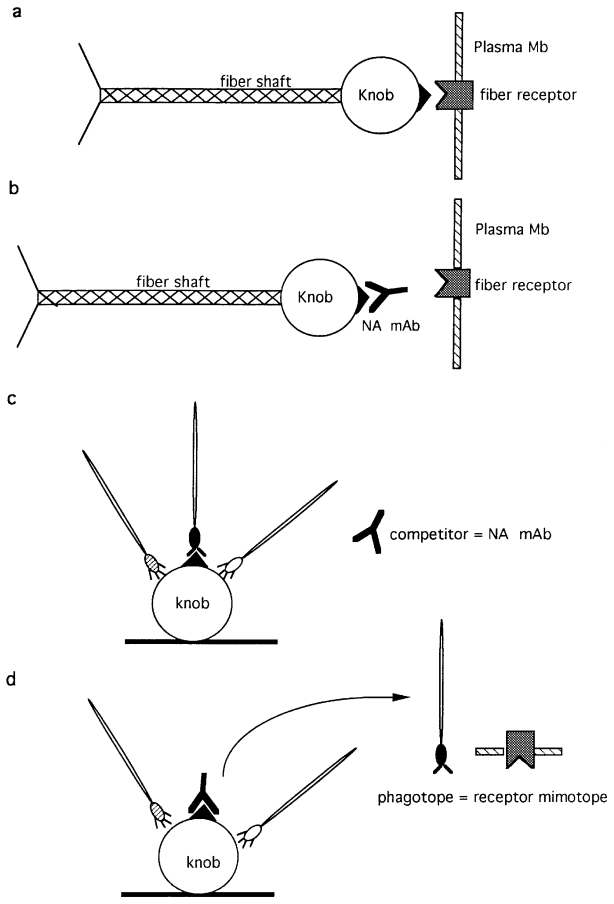

Fig. 1. Strategy for identifying Ad5 fiber knob receptor using biopanning of a phage-displayed hexapeptide library on immobilized recombinant knob protein, and neutralizing anti-knob mAb. (**a**) Fiber knob-mediated binding of Ad particle to the fiber receptor on the membrane of susceptible cells. (**b**) Inhibition of Ad–cell attachment by a neutralizing (NA) mAb binding to an epitope (represented by a black triangle) localized in the knob domain. (**c**) Biopanning of a library of recombinant phages carrying random hexapeptides in the pIII attachment protein. (**d**) Specific displacement of phages by the NA mAb used as competitor yields phage species carrying phagotopes which are mimotopes of cell receptor peptide motifs.

depicted in Figure 1, phages first adsorbed to immobilized Ad5 knob recombinant protein were eluted using each mAb as a competing ligand. The phage motifs thus obtained essentially represented mimotopes of knob-binding domains of cell membrane proteins. Two classes of ubiquitous motifs were therefore identified. The first class was consensus to the human fibronectin type III (FNIII) module previously identified (Hong and Boulanger, 1995); the second had strong homology with a conserved segment of the α2 domain of heavy chains of human major histocompatibility complex class I molecules (MHC-I α2) (Bjorkman and Parham, 1990), overlapping tryptophan residue 167 near the peptide-binding site. When expressed in fusion with GST, both FNIII- and MHC-I α2-derived motifs showed an Ad5 and Ad2 (but not Ad3) fiber knob-binding capacity *in vitro*. In *in vivo* assays, synthetic icosapeptide RAIVGFRVQWLRRYFVNGSR, representing the MHC-I α2 segment, efficiently neutralized Ad5 and Ad2 (but not Ad3), whereas RHILWTPANTPA-MGYLARVS, representing the FNIII consensus motif, significantly enhanced Ad5 cellular attachment. Our data suggest that a segment of MHC-I α2, which is conserved between all HLA alleles, is involved in the primary binding of Ad5 to HeLa cells (fiber receptor), and that FNIII modules carried by other membrane components would act as auxiliary receptors or binding co-factors.

Results

mAbs 1D6.3 and 7A2.7 blocked the attachment of Ad5 to HeLa cells

The reactivity of 1D6.3 and 7A2.7 against recombinant fiber knobs expressed in insect cells was first analyzed by enzyme-linked immunosorbent assay (ELISA). They were found to react with native Ad5 knob (F5-AT386), but not with SDS-denatured F5-AT386 or with Ad2 or Ad3 knobs (not shown), suggesting that they recognized serotype-specific and conformation-dependent epitopes. Both 1D6.3 and 7A2.7 neutralized Ad5 with a high efficiency (data not shown). In a former antigenic analysis of Ad2 fiber (Watson *et al.*, 1988), it has been reported that two anti-knob neutralizing mAbs out of 14 failed to inhibit Ad2-induced hemagglutination, implying that neutralization by anti-knob antibodies could result from several mechanisms, and not only from inhibition of virus attachment.

In order to determine whether the Ad5 neutralization effect was due to blocking at the fiber knob receptor-binding site, 1D6.3 and 7A2.7 were tested for their inhibitory effect on Ad5–cell attachment. This was carried out using ^{14}C-labeled Ad5 virions in a microbinding assay with *in situ* autoradiography of virus-exposed HeLa cells (Figure 2a–d), and in a conventional binding assay with counting cell-adsorbed radioactivity (Figure 2e). In the presence of irrelevant mAb (Figure 2a), a dark halo of reduced silver grains was visible around the cells on which virions had adsorbed. This was expected, since the ^{14}C isotope is a relatively high energy photon emitter (Masse, 1976). In the presence of mAb 1D6.3 or 7A2.7, the number of silver grains associated with and around the cells decreased in a mAb concentration-dependent manner (Figure 2b–d), a result confirmed by the cell-bound radioactive counts (Figure 2e). 1D6.3 was slightly more efficient than 7A2.7 in virus-binding inhibition at the same mAb concentration (Figure 2e). These results indicated that neutralization of Ad5 by 1D6.3 and 7A2.7 resulted from the specific blockage of virus–cell attachment, and not from the inhibition of an intracellular event.

Identification of the 1D6.3 and 7A2.7 epitopes on the fiber knob

Since peptide scanning has been found to be inadequate to map conformational epitopes in fiber knobs (Fender *et al.*, 1995), a phage-displayed hexapeptide library was biopanned on the anti-knob mAbs, and the hexapeptide motifs (phagotopes) carried by the eluted phages were determined by DNA sequencing. Although mAbs 1D6.3 and 7A2.7 reacted with conformation-dependent epitopes, we assumed that there would be sufficient contiguous amino acids in the phagotopes to be able to recognize specific motifs in the Ad5 knob sequence, as previously found for penton base mAb (Hong and Boulanger, 1995). As shown in Figure 3, mAbs 1D6.3 and 7A2.7 behaved as two independent clones, which mapped to two adjacent

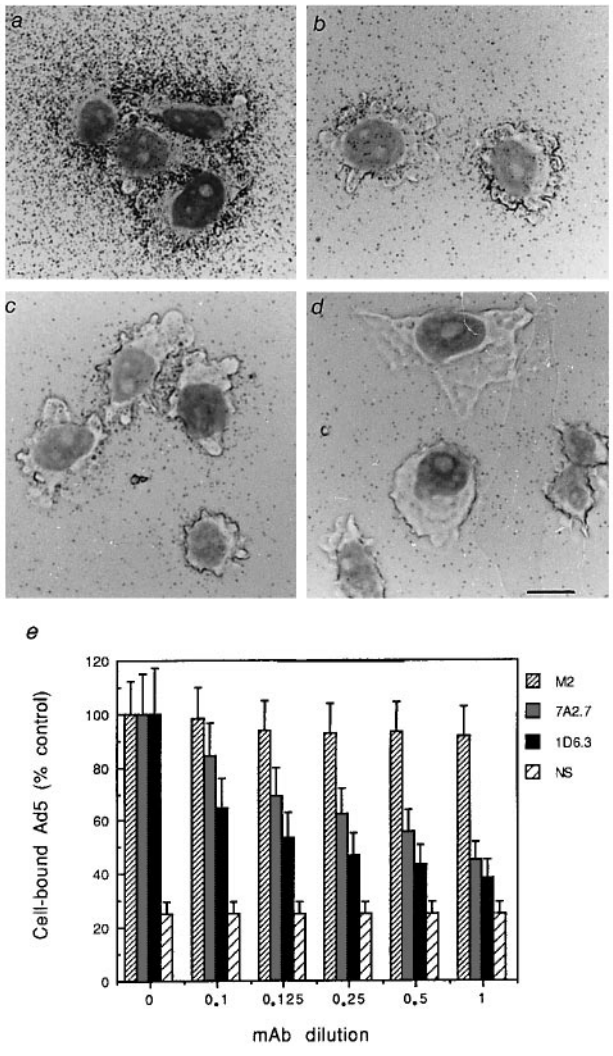

Fig. 2. Inhibition assay of attachment of labeled Ad5 virions to HeLa cell surface by anti-knob mAbs. (**a**–**d**) *In situ* autoradiography of cell-bound [^{14}C]Ad5, after incubation at 0°C for 1 h in the presence (b–d) of mAb 1D6.3, used as hybridoma cell culture fluid at the following dilutions, 1:10 (b), 1:4 (c) and 1:2 (d). (a) Control, irrelevant mAb (anti-FLAG M2) used at 0.1 μg/ml in hybridoma cell culture medium. Note that, as a relatively high energy photon emitter compared with ^{3}H, the ^{14}C isotope has a maximum path emission of 96 μm in photographic emulsion, which explains the occurrence of reduced silver grains at a distance from the cell contour. Bar indicates 10 μm. (**e**) Liquid scintillation counting of cell-attached radioactive virus. Aliquots of Ad5 virions (10^5 c.p.m.) were adsorbed to 10^5 HeLa cells at 0°C for 1 h, in the presence of increasing concentrations of mAb 7A2.7, 1D6.3 or irrelevant mAb M2. Results were expressed as the percentage of virus adsorbed to cells in the absence of mAb (corresponding to ~5% of the total radioactivity input). Non-specific binding (NS) was evaluated by chasing labeled virus by a 50-fold excess of unlabeled virus (Defer *et al.*, 1990; Wickham *et al.*, 1993). This represented as much as 25% of the cell-bound virus. The values represented the average of three separate experiments in triplicate.

segments spanning 15–20 amino acid residues in the knob linear sequence.

mAb 1D6.3 retained a variety of peptide phagotopes with overlapping residues, spanning the knob region between Val438 and Asp462. In spite of a certain degree of degeneration and scatter, a core motif, ^{445}LAPISGTVQ-SAHLIIRFD^{462}, centered on the bulky histidine residue at position 456, could be identified. Histidine was found repeatedly in several independent phage clones. Moreover, three phagotopes contained a histidine next to a serine (GISHTG and GASHTV), and a homologous sequence was found in the Ad5 knob, as ^{453}QSAHLI^{458}. On the N-terminal side of this peptide sequence, the motif LAPIS was represented in several phagotopes as L-P, VAP-S and LIPF(N)S. In the Ad2 fiber knob, a similar region, within residues 459–470, has also been identified as an Ad2 neutralization domain (Fender *et al.*, 1995).

Likewise, the 7A2.7 epitope was mapped to the region within residues 473–486, ^{473}LDPEYWNFRNGDLT^{486}. From the sequence analysis, proline was represented four times and tryptophan and histidine eight times out of 15 phagotopes, and association of two aromatic residues in the same phagotope was found five times (Figure 3). It seemed, therefore, that in the 7A2.7 epitope, a proline residue, such as P475, would be in the close vicinity of a cluster of aromatic residues, such as ^{477}YWNF^{480}. In addition, two phagotopes, FWLAVR and WALFRS, were found to be homologous to the Ad5 knob motif ^{477}YWNFR^{481}.

According to the fiber knob three-dimensional model recently proposed (Xia *et al.*, 1994), both epitopes occupy spatially contiguous regions. The 1D6.3 epitope spanned part of the CD loop and the β-strand D, whilst the 7A2.7 epitope was localized to the adjacent segment DE and the two β-strands E and F. The 1D6.3 epitope falls within the R-sheets, i.e. the knob domain facing the cell receptor (Xia *et al.*, 1994), while the 7A2.7 epitope is oriented more laterally from the R-sheets.

Elution of phages from the fiber knob by competition with mAbs

The phage library was biopanned on immobilized Ad5 fiber knob, and knob-adsorbed phages were then eluted using 1D6.3 and 7A2.7 as soluble competitors in reverse ligand elution (Hong and Boulanger, 1995). The hexapeptide motifs identified belonged to two distinct classes (Figure 4).

The phagotopes yielded by competition with 7A2.7 had homology with motifs already isolated by biopanning on recombinant Ad2 fiber (Hong and Boulanger, 1995), and identified as consensus to peptide sequences of the human FNIII modules (Main *et al.*, 1992; Dickinson *et al.*, 1994). For example, ILWTPG, WYEWIG and WVIWSI, found in the 7A2.7 eluate (Figure 4a), were homologous to GLSIWN, FSWLVI, WSIAVS and WWVIRD, recovered by acid elution from full-length fiber and fiber knob. Thus, the partially overlapping motifs of the 7A2.7-displaced phagotopes represented a sequence consensus to the β-strand B and adjacent BC loop of the FNIII module (Dickinson *et al.*, 1994). The peptide ILWTPG was homologous to IMWTP found in FNIII module 4, LQYSLP to IQWNAP present in module 1, and RHWPF to RWTPP found in module 5 (Figure 4a).

The second class of peptide motifs, found in the 1D6.3 eluate, showed a pattern of overlapping sequences which formed the consensus tetracosapeptide ARAIVGFRVQW-LRRYFVNGSRETI (Figure 4b). The search for homology of this 1D6.3-displaced peptide motif to other reported sequences in data banks revealed that it had 64% identity with the C-terminal portion of the human MHC-I α2 in a 14 residue overlap between Gly162 and Gly175 comprising Trp167, and 77% homology in a 22 residue overlap

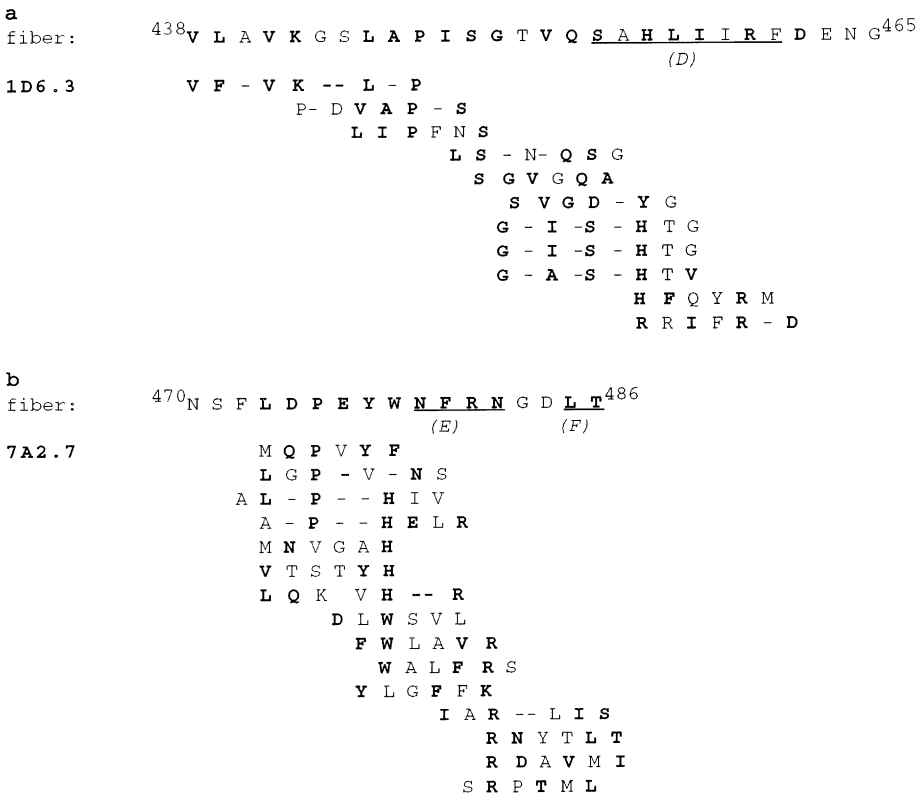

Fig. 3. Phagotopes recovered from biopanning of mAbs 1D63 (**a**) and 7A2.7 (**b**). The phagotope motifs are aligned with the corresponding knob sequence, residues of which are numbered from the initiator methionine of full-length Ad5 fiber. Regions in β-sheet structure (Xia *et al.*, 1994) are underlined and marked by *(D)*, *(E)* and *(F)*. Identical or conserved residues in the sequences are indicated in bold face.

between Arg157 and Leu179 (Figure 4b). Some of the peptides isolated have already been identified as ligands of the Ad2 fiber (Hong and Boulanger, 1995), such as DRRYMP, which is homologous to RRYFVN found as the core motif of the MHC-I α2 consensus region.

Interactions of Ad fibers with FNIII module and MHC-I α2 in vitro and serotype specificity of the binding

To analyze further the possible role of FN and MHC class I molecules in fiber knob recognition, oligopeptide sequences homologous to the FNIII modules and MHC-I α2 domains were fused to GST, and used in *in vitro* binding assays with recombinant knobs and full-length fibers from different Ad serotypes. Thus, the pentadecapeptide RHILWTPANTPAMGY, homologous to the β-strand B and adjacent BC loop of the human FNIII module (Dickinson *et al.*, 1994), was fused to the oligoglycine linker at the C-terminus of GST, in single (GST–FN×1) or multiple (GST–FN×2 and GST–FN×3) motifs in tandem. Likewise, the icosapeptide RAIVGFRVQWLRRYFVNGSR, which was consensus to the sequence of the MHC-I α2 within residues 157–176 (Bjorkman and Parham, 1990), was fused to GST, and the resulting fusion proteins were referred to as GST–MHC×1, GST–MHC×2 and GST–MHC×3, according to the number of copies of inserted motif.

The different fusion proteins were incubated *in vitro* with recombinant fiber knobs of serotypes 5 (F5-AT386), 2 (F2-AT388) and 3 (F3-AT124) respectively, and complexes, isolated by affinity to glutathione–agarose beads, were analyzed by SDS–PAGE and immunoblotting. GST–FN×1, GST–FN×2 and GST–FN×3 were found to bind to F5-AT386 and F2-AT388 proteins with a high efficiency, whereas F3-AT124 was retained at much lower levels (not shown). A similar pattern was observed with GST-fused MHC-I α2-derived oligopeptides GST–MHC×1, GST–MHC×2 and GST–MHC×3, which retained F5-AT386 and F2-AT388 in significantly higher yields than F3-AT124 (not shown).

In vitro binding assays were also performed using recombinant full-length fibers of Ad5 (F5-FL581), Ad2 (F2-FL582) and Ad3 (F3-FL320). The amount of GST–oligopeptide-bound fiber could be quantitated in immunoblot by using anti-fiber tail mAb 4D2.5 (Hong and Engler, 1991), since the 4D2.5 epitope, FNPVYP, determined by phage biopanning (Hong and Boulanger, 1995), is totally conserved between Ad serotypes 5, 2 and 3, and in most of the mammalian Ad serotypes (Chroboczek *et al.*, 1995). As shown in Figure 5, Ad5 fiber bound to GST–MHC and GST–FN fusion proteins with a significantly higher affinity than Ad2 fiber (2- to 3-fold), and with a 10- to 15-fold higher efficiency than Ad3 fiber. The efficiency of binding of recombinant fiber to GST-fused MHC- or FNIII-derived peptides did not increase in parallel to the number of motifs present in the fusion protein, and, in some cases, slightly decreased between one single and two or three motifs in tandem (Figure 5). This suggested that in some constructs, tandem motifs could adopt a conformation which was detrimental to the knob binding, and that only one single molecule of fiber could bind per GST-fused oligopeptide bait provided to the incubation

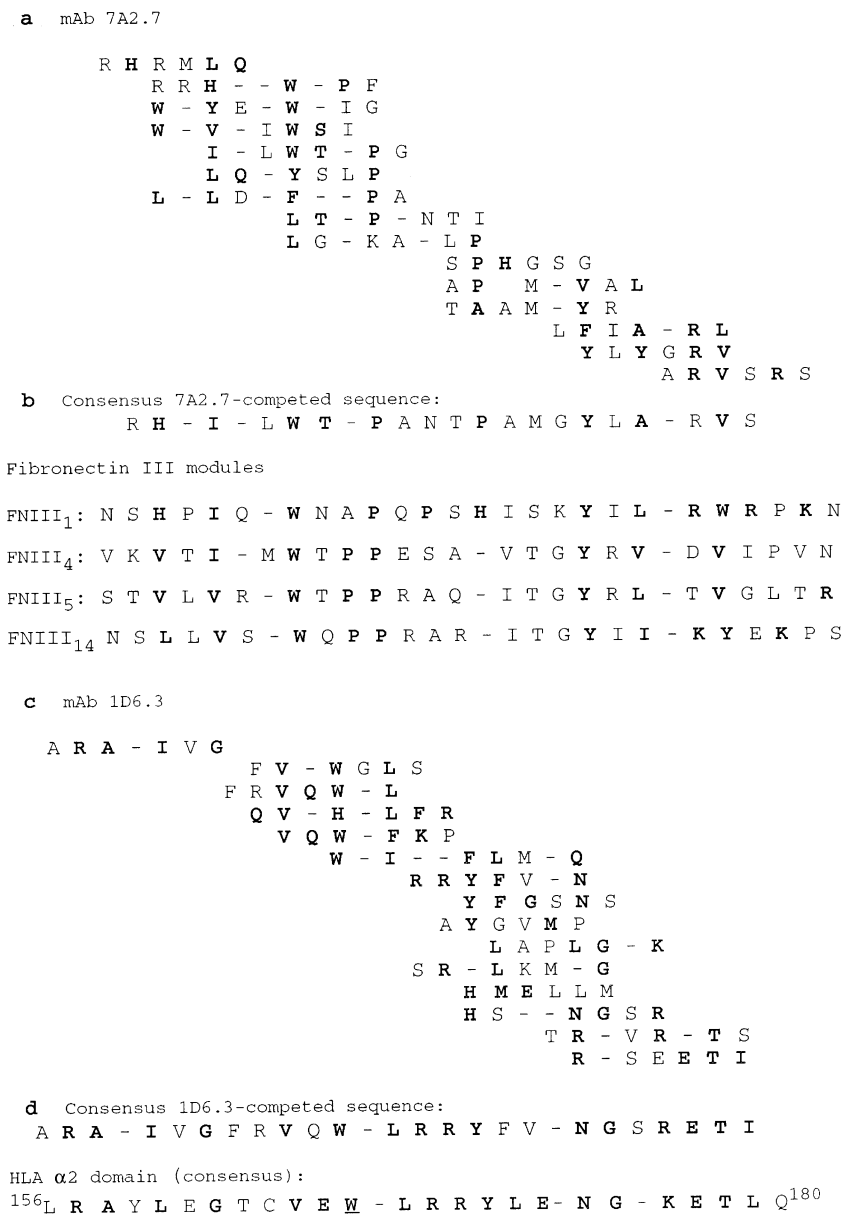

Fig. 4. (**a**) mAb 7A2.7-competed phagotopes, and (**b**) sequence alignment of consensus 7A2.7-eluted sequence with some FN type III modules (Dickinson *et al.*, 1994). (**c**) 1D6.3-competed phagotopes, and (**d**) consensus 1D6.3-eluted sequence, tentatively aligned with the consensus MHC class I heavy chain α2 domain (Bjorkman and Parham, 1990) around tryptophan residue 167 (underlined). Conserved residues at analogous positions are in bold face. Hyphens were introduced to maximize the alignment.

mixture, probably due to steric hindrance of the bulky knob domain.

Binding of Ad5 fiber monomer to GST-fused FNIII- and MHC-I α2-derived peptides

Fiber mutant F5-*dl*314–402, carrying a 90 amino acid deletion spanning the shaft and the shaft–knob junction (including the conserved TLWT motif; Chroboczek *et al.*, 1995), occurred in monomeric form when expressed as recombinant protein in baculovirus-infected cells (our unpublished data). Recombinant fiber mutant F5-*dl*314–402 was thus tested for its ability to bind to GST-fused FNIII- and MHC-I α2-derived peptides. Both fusions were found to bind to the F5-*dl*314–402 mutant *in vitro* with almost the same efficiency as wild-type Ad5 fiber (Figure 5). This implied that the FNIII module and the MHC-I α2 had similar affinity for fiber knob monomers and trimers, suggesting that they did not recognize trimer-dependent peptide motifs.

Interference of FNIII- and MHC-I α2-derived synthetic peptides with Ad5 in vivo

Two icosapeptides, RHILWTPANTPAMGYLARVS (FN20) and RAIVGFRVQWLRRYFVNGSR (MH20), which reproduced the consensus sequence of 7A2.7- and 1D6.3-eluted phagotopes, respectively (Figure 4), were synthesized and assayed for their effect on Ad5Luc3 cellular attachment and subsequent luciferase gene expression. Luciferase activity in Ad5Luc3-infected cell extracts was plotted versus the m.o.i., at various icosapeptide concentrations (Figure 6). The slope of the different regression lines increased progressively with increasing

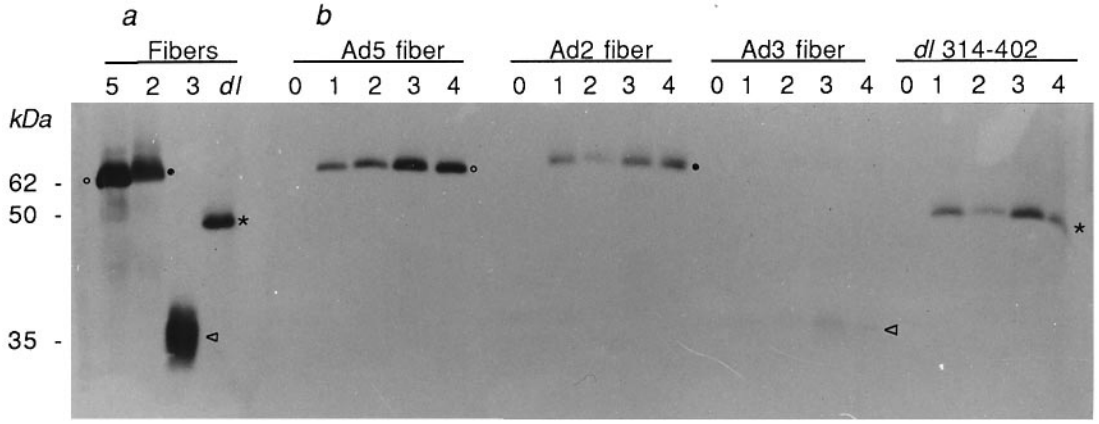

Fig. 5. Serotype-specific binding of Ad fibers to GST-fused FNIII- and MHC I α2-derived peptides *in vitro*. (**a**) Control lanes showing recombinant fibers of Ad5 (5), Ad2 (2), Ad3 (3) and F5-*dl*314–402 mutant (*dl*) used in binding assays, with their apparent molecular masses given in kDa on the left. (**b**) Lanes (0), control, unfused GST; lanes (1), GST–FN×1; lanes (2), GST–FN×3; lanes (3), GST–MHC×1; lanes (4), GST–MHC×3. The blot was reacted with anti-fiber tail domain 4D2.5 mAb. The position of GST fusion-bound recombinant fibers is indicated by an open dot for Ad5, solid dot for Ad2, open arrowhead for Ad3 and asterisk for F5-*dl*314–402, respectively.

FN20 molarities, with a 5-fold increase at 50 μM compared with 5 μM, and a 20-fold increase between 5 and 100 μM (Figure 6a). By contrast, MH20 showed an apparent 4-fold augmentation of luciferase activity at 5 μM, but an almost total abolition of the enzyme expression at 25 μM (Figure 6b).

The biological effects of FN20 and MH20 were then analyzed at increasing peptide molarities and constant m.o.i. (0.16 f.f.u./10^5 cells), a m.o.i. value chosen in the linear range of virus dose–luciferase response (refer to Figure 6). For FN20, no significant effect was observed for molarities up to 10 μM, but a progressive increase in luciferase activity occurred over 25 μM, with a 100-fold increase between 25 and 500 μM (Figure 7a). With MH20, there was a discrete augmentation of luciferase gene expression for molarities ranging from 0.05 to 2.5 μM, with a 5- to 6-fold higher level at 2.5 μM. This was followed by a rapid decrease of luciferase levels for molarities >5 μM, with a four orders of magnitude lower level than the control samples at 50 μM (Figure 7b). There was no apparent cytotoxicity of the two peptides in the molarity range used.

The fact that there was no significant influence of MH20 and FN20 peptides on Ad5Luc3 transgene expression, once the virus was pre-attached or pre-endocytosed (Figure 7a and b), suggested that the observed effects occurred at the attachment step. In addition, the enhancing effect of FN20 on Ad5Luc3 expression was reproduced in a fiber–HeLa cell binding assay, using recombinant Ad5 fiber and anti-tail mAb 4D2.5 in flow cytometry analysis (data not shown).

The almost total inhibition of luciferase expression at 50 μM MH20 implied a strong virus neutralization effect. This was confirmed by the MH20 blockage of adenovirion structural protein synthesis. When HeLa cells were infected with wild-type Ad5 or Ad2 at a m.o.i. ranging from 0.2 to 2.0 f.f.u./cell in the presence of 25 μM MH20 during the phase of virus attachment, a 15- to 30-fold decrease in the synthesis of the major capsid proteins hexon, 100K, penton base and fiber was observed at 48 h after infection. At the same MH20 molarity, only a 1.5- to 2-fold reduction was obtained with wild-type Ad3 (Figure 8). This suggested that Ad neutralization by MH20 occurred in a serotype-dependent manner.

Affinity of Ad5 fiber for FNIII- and MHC-Iα2-derived synthetic peptides

^{35}S-labeled recombinant fiber F5-FL581 was titrated down a series of icosapeptide-coated microtitration wells. A dissociation constant (K_d) of 3.0 ± 0.6 nM was found for MH20 and 8.0 ± 1.9 nM for FN20 (n = 3), as derived from classical Scatchard analysis (Scatchard, 1949). Values of 1.7 nM (Wickham *et al.*, 1993) and 2.0 nM (Hong and Boulanger, 1995) have been reported for the K_d of the recombinant fiber and HeLa cell binding reaction.

MHC class I dependence of Ad5 attachment to human B lymphoblastoid cells

Daudi cell, an established B lymphoblastoid Burkitt's lymphoma cell line, is deficient in the expression of β_2-microglobulin, and thus lacks HLA class I molecules at its surface (Daudi-HLA$^-$). A Daudi-derived cell line (E8.1), which has been transfected with the β_2-microglobulin gene, expresses functional HLA class I at its surface (Daudi-HLA$^+$; Quillet *et al.*, 1988). Both Daudi-HLA$^-$ and Daudi-HLA$^+$ were assayed for attachment of radiolabeled Ad5. Ad5 was found to bind to Daudi-HLA$^+$ cells with a 10-fold higher efficiency than to Daudi-HLA$^-$ cells. The saturation curve obtained at 0°C showed a discrete sigmoidal curvature suggestive of some cooperative binding (Figure 9a). The Scatchard plot of the binding data with Daudi-HLA$^+$ confirmed the cooperativity (Figure 9b). The values for the apparent association constant, K_a, ranged from 0.9×10^{10} to 2.3×10^{10}/M, with an average of $1.4 \pm 0.6\times10^{10}$/M (K_a ± SD; n = 4) in terms of Ad5 molarity. This value was similar to the binding constants reported for Ad2 and HeLa (Persson *et al.*, 1985; Seth *et al.*, 1994) or KB cells (Defer *et al.*, 1990). The intersection with the x-axis gave 4000 ± 500 receptors per cell, a value slightly lower than the number of Ad2 receptors at the surface of HeLa or Cos-7 cells, 10 000 and 12 000, respectively (Persson *et al.*, 1985; Seth *et al.*, 1994).

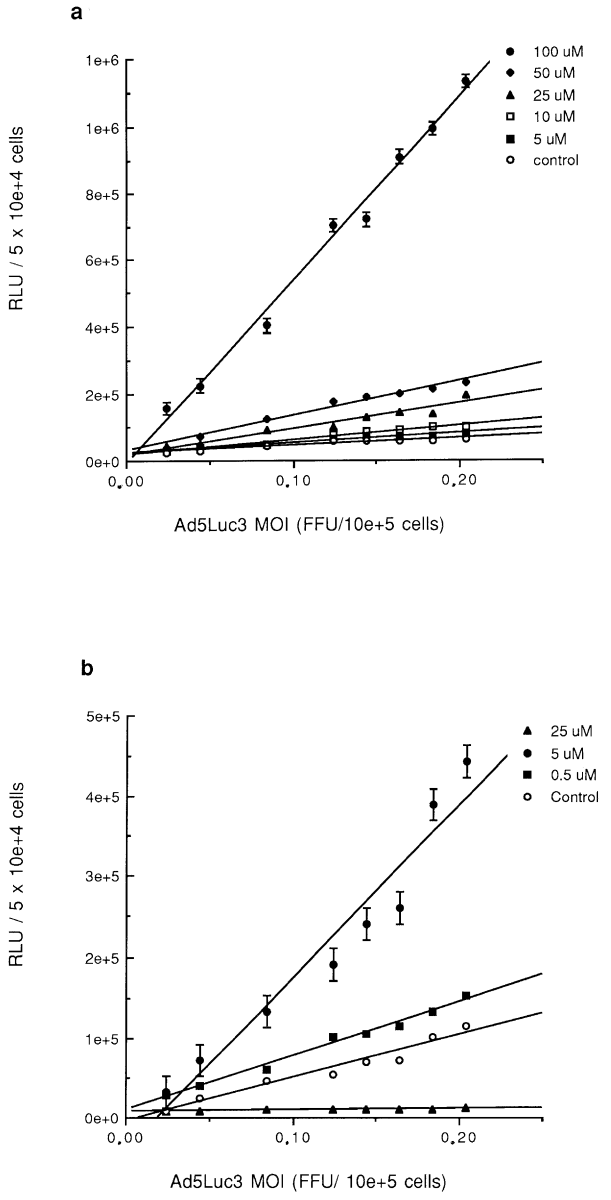

Fig. 6. Dose–response of luciferase activity (expressed as relative light units; RLU) in HeLa cells (10^5 cells) infected with Ad5Luc3 at varying m.o.i. in the absence (control unrelated peptides, ○), or presence of (**a**) FN20 peptide at increasing molarities (5, 10, 25, 50 and 100 μM), or (**b**) MH20, at 0.5, 5 and 25 μM. Ad5Luc3 and peptides were incubated with cell monolayers at 0°C, a temperature which only allows virus–cell attachment but not entry. Unadsorbed virus was rinsed off, and the cells further incubated at 37°C for 18 h and processed for luciferase assays. Values shown represent the average of three separate experiments.

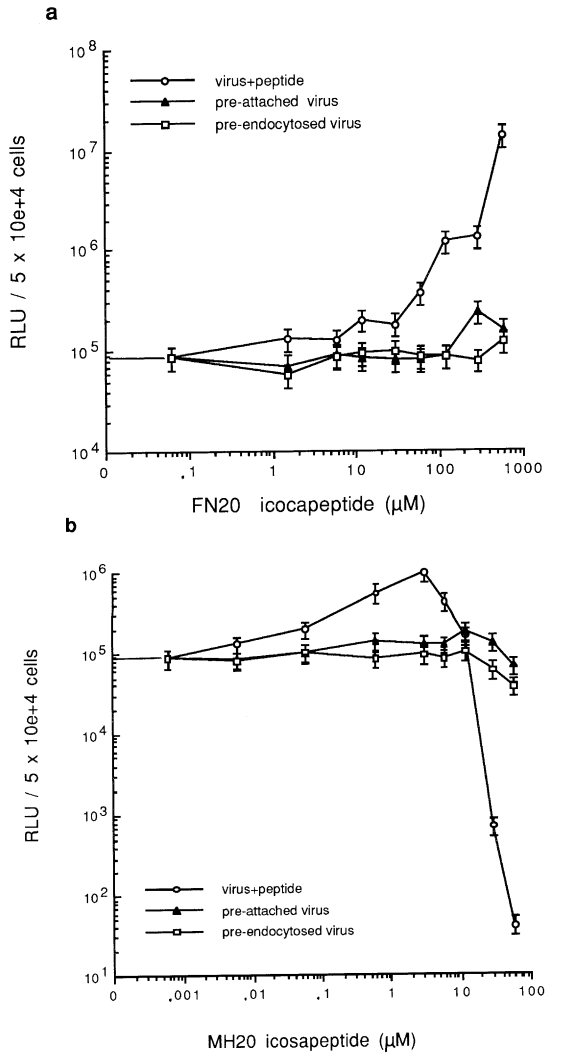

Fig. 7. Luciferase gene expression in HeLa cells infected with Ad5Luc3 at constant m.o.i. (0.16 f.f.u./10^5 cells), and in the linear range of RLU versus m.o.i. as determined in Figure 6. Ad5Luc3 was added to the cells pre-cooled at 0°C in the presence of increasing molarities of (**a**) FN20, ranging from 0 to 500 μM, or (**b**) MH20, ranging from 0 to 50 μM. Control curves corresponded to luciferase activity in HeLa cells incubated with FN20 or MH20 after Ad5Luc3 attachment (▲), or after Ad5Luc3 endocytosis (□). In (b), the luciferase level detected at 50 μM MH20 represents the background activity in mock-infected HeLa cells (~50 RLU per 5×10^4 cells).

Functionality of Ad5 receptors in Daudi-HLA$^+$ cells

In order to determine whether the receptor sites present on Daudi-HLA$^+$ cells were functional in terms of virus life cycle, and could lead to virion endocytosis, nuclear transport and expression of the viral genome, Ad5Luc3 was adsorbed to Daudi-HLA$^+$ cells at 0°C and at increasing m.o.i., and luciferase assayed in cell lysates at 18 h after the temperature shift-up. As shown in Figure 10, the luciferase activity in Daudi-HLA$^+$ followed the Ad5Luc3 m.o.i. in a dose-dependent manner, and reached a plateau at >5 f.f.u./10^5 cells. The luminescent signal obtained with Daudi-HLA$^-$ was 3–4 orders of magnitude lower than with Daudi-HLA$^+$ cells.

To test whether the Ad susceptibility of Daudi-HLA$^+$ cells directly depended upon cell surface expression of HLA class I molecules, and not other cellular molecules co-transported to the plasma membrane, Ad5Luc3 was incubated with Daudi-HLA$^+$ cells at 0°C and 10 f.f.u./10^5 cells in the presence of various amounts of peptide MH20. The luciferase signal decreased progressively with increasing molarities of MH20, showing 50% inhibition at 40 μM, and 88% inhibition at 100 μM (data not shown), which confirmed the role of HLA class I molecules in Ad5Luc3 binding to Daudi-HLA$^+$ cells.

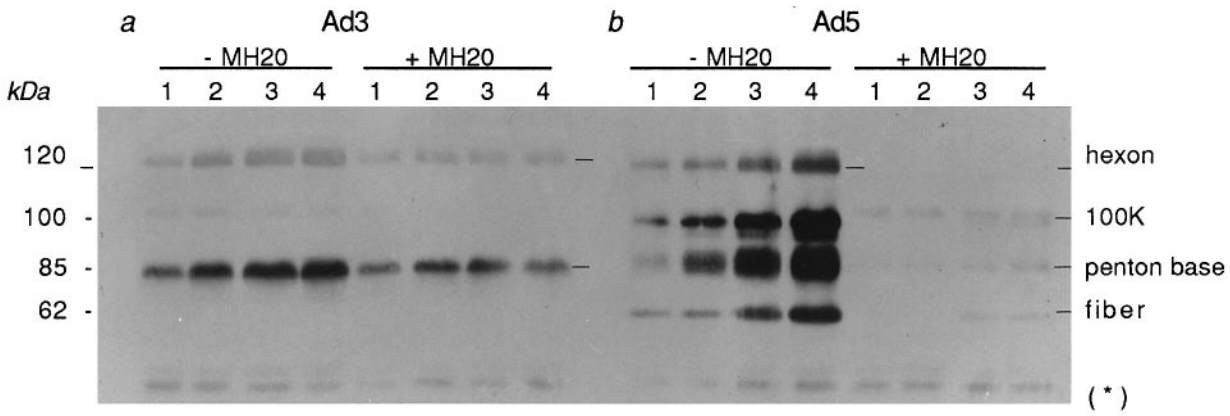

Fig. 8. Serotype specificity of virus neutralization by MH20 peptide. Wild-type Ad3 (**a**) or Ad5 (**b**) were pre-incubated in the absence (–) or presence of (+) MH20 at 25 μM for 2 h at room temperature, and the mixture added to pre-cooled HeLa cells (10^5 cells) at varying m.o.i., ranging from 0.2 (lanes 1), 0.5 (lanes 2), 1.0 (lanes 3) to 2.0 (lanes 4) f.f.u./cell, for 1 h at 0°C. Unadsorbed virus was rinsed off and cells transferred to 37°C for 48 h. Late structural proteins, hexon (apparent M_r 120 kDa for its subunit), hexon-scaffold protein 100K (100 kDa), penton base (85 kDa) and fiber (62 kDa) were then analyzed by SDS–PAGE and immunoblotting using rabbit anti-Ad2 virion serum. This serum reacts with group- and subgroup-specific determinants present in hexon, 100K, penton base and fiber of Ad2 and Ad5, and group-specific determinants of Ad3 hexon and penton base (Boudin and Boulanger, 1982). Note the net neutralization activity of MH20 towards Ad5, compared with its discrete down-effect on Ad3. (*), cellular protein band non-specifically detected by the secondary antibody.

Discussion

Two mAbs raised against recombinant Ad5 fiber knob, 7A2.7 and 1D6.3, were found to neutralize Ad5 infection of HeLa cells via inhibition of virus attachment to the cell surface (Figure 2). They were thus used as immunological probes for fiber receptors, considered as the primary cell receptors of the virion (White, 1993). Their epitopes, identified by biopanning of a phage-displayed random hexapeptide library, were mapped to a region of the terminal knob spanning residues 438–486 in the fiber sequence (Figure 3). This corresponded to the CD loop and the D floor for 1D6.3, the adjacent DE segment and β-strands E and F for 7A2.7 (Xia *et al.*, 1994). The same region of the knob has been proposed to be involved in Ad2 neutralization by anti-Ad2 fiber knob mAbs which recognize conformational epitopes (Fender *et al.*, 1995). The β-strand D, included in the 1D6.3 epitope, has been assigned to the R-sheets of the knob which face the cell receptor (Xia *et al.*, 1994).

Specific displacement of phages bound to immobilized Ad5 knob by 1D6.3 or 7A2.7 used as competing ligands yielded phagotopes which represented mimotopes of fiber knob-binding proteins (Figure 1). The mimotopes identified belonged to two distinct classes of ubiquitous cellular protein motifs. The phagotopes competed by 7A2.7 (Figure 4a) showed significant homology to motifs which have been isolated previously from Ad2 fiber, and identified as consensus to a region of human FNIII modules (Hong and Boulanger, 1995) corresponding to the β-strand B and adjacent BC loop (Main *et al.*, 1992; Dickinson *et al.*, 1994). In the 1D6.3 eluate, the pattern of overlapping phagotopes represented a consensus sequence which had 77% homology (17 identical or conserved residues out of 22) with the C-terminal portion of the human MHC- I α2 molecules, including Trp167 (Figure 4b). Little variability has been found in this particular region of the α2 domain among all HLA alleles (Bjorkman and Parham, 1990; Messer *et al.*, 1992), and this accessible and conserved segment corresponds to a portion of the peptide-binding α-helices (Bjorkman and Parham, 1990). When fused to bacterially expressed GST protein, both FNIII module-derived and MHC-I α2-derived consensus oligopeptide sequences bound efficiently *in vitro* to recombinant fibers of Ad5 and Ad2, but not to fiber of Ad3 (Figure 5). Their capacity to bind to the recombinant shaft mutant F5-*dl*314–402, which failed to trimerize and accumulated as fiber monomers, suggested that the recognition of the FNIII module and MHC-I α2 by the Ad5 fiber knob was not trimer dependent.

Two icosapeptides were synthesized: MH20, which represented the consensus mimotope of the MHC-I α2, and FN20, which represented the consensus mimotope of the FNIII module (Figure 4). Immobilized MH20 was found to bind to recombinant Ad5 fiber with a K_d of ~3 nM, a value which was close to the previously reported K_d for the binding reaction of recombinant fiber to HeLa cell receptors (1.7–2.0 nM; Wickham *et al.*, 1993; Hong and Boulanger, 1995).

When assayed *in vivo* in HeLa cell binding competition with Ad5Luc3, FN20 showed no significant biological effect for molarities up to 10 μM, but a progressive augmentation of Ad5Luc3 attachment was observed at molarities >25 μM. The paradox of the positive effect of FN20, a peptide which was derived from the neutralizing mAb 7A2.7, is apparent: (i) the lateral position of the 7A2.7 epitope on the knob structure (Xia *et al.*, 1994), compared with 1D6.3, is compatible with a function of binding to an auxiliary ligand; (ii) on the other hand, the 7A2.7 antibody molecules bound to their epitopes on the knob could impair, by steric hindrance, its attachment to the cell receptor. With MH20, the curve of biological activity was found to be biphasic: (i) at low molarities, an initial increase in the luciferase gene expression was observed, up to 5-fold at 2.5 μM; (ii) at higher molarities, between 10 and 25 μM, a negative effect was detected, followed by complete virus neutralization at 50 μM (Figures 6 and 7). This curve suggested some cooperativity of MH20 for the binding of the virus to its cell receptors. A discrete positive cooperative effect in Ad–cell binding has already been described (Persson *et al.*, 1985; Defer

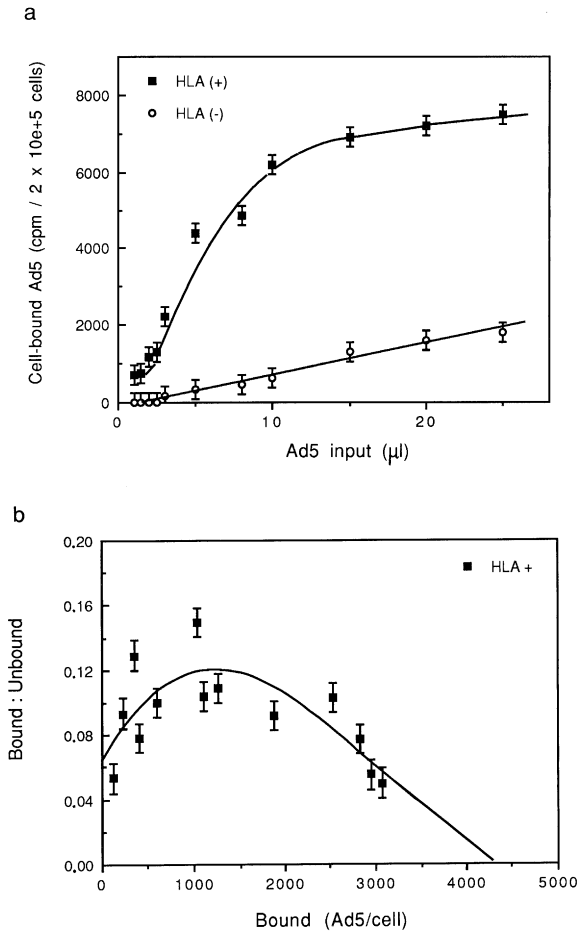

Fig. 9. Binding reaction and titration of Ad5 receptor sites at the surface of parental Daudi-HLA$^-$ and β_2-microglobulin-transformed Daudi-HLA$^+$ cells. (**a**) Increasing amounts of [^{3}H]thymidine-labeled Ad5 (6000 c.p.m./µl; 5×10^8 virions/µl) were incubated with cells (2×10^5 per sample) at 0°C for 1 h in a total volume of 100 µl of PBS. Cell-bound radioactivity was counted in a liquid spectrometer. (**b**) Scatchard plot analysis of the binding reaction of Daudi-HLA$^+$ cells, as shown in (a). Note the sigmoid shape of the curve in (a) and the upward curvature of the corresponding plot in (b), suggesting a positive cooperative effect in the Ad5–receptor binding process.

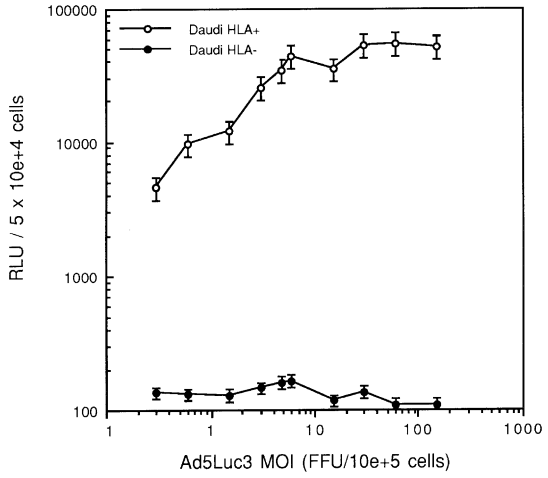

Fig. 10. Functionality of Ad5 receptors in Daudi-HLA$^+$ cells. Luciferase gene expression in Daudi-HLA$^-$ and Daudi-HLA$^+$ cells infected with Ad5Luc3 at varying m.o.i. (0.3–150 f.f.u./10^5 cells). Ad5Luc3 was added to the cells pre-cooled at 0°C for 1 h to allow virus attachment but not entry. After rinsing unadsorbed virus, the cells were resuspended in medium pre-warmed to 37°C, further incubated at 37°C for 18 h, then processed for luciferase assay. RLU values represent the average of three separate experiments with Daudi-HLA$^-$ (●) and Daudi-HLA$^+$ (○).

et al., 1990). Since fiber is a trimer, this would imply that the binding of MH20 peptide to one or two monomers of the knob could facilitate the binding of the last free knob monomer site to its cell receptor.

In virus neutralization assays, MH20 showed an efficient neutralization of Ad5 and Ad2, but not of Ad3 (Figure 8). The serotype specificity of Ad neutralization by MH20 peptide, as well as the serotype specificity of the *in vitro* interactions between fibers and GST–MHC-I α2 peptides (Figure 5) was consistent with previous studies showing that Ad2 and Ad5 share the same receptor, which is different from the Ad3 receptor (Defer *et al.*, 1990; Stevenson *et al.*, 1995). In the range of molarities of the two peptides used, no apparent cytotoxicity or inhibition effect on the expression of pre-attached or pre-endocytosed Ad5Luc3 was observed (Figure 7). This, and the fact that our assays were conducted at 0°C, a temperature which permits only virus attachment and not cell entry, implied that the observed biological effects occurred at the stage of virus attachment, and, more specifically, the binding of the knob to the fiber receptor.

Our results suggest that the region confined to the CD loop, D strand, DE segment and EF β-strands of the Ad5 fiber knob recognizes at least two distinct HeLa cell plasma membrane ligands: (i) the MHC-I α2, and (ii) another, as yet unidentified, membrane protein containing one or several copies of the promiscuous FNIII module. MHC class I molecules have been found to serve as receptors for several viruses, including SV40 (Breau *et al.*, 1992), mouse cytomegalovirus, lactate dehydrogenase virus and Semliki Forest virus (reviewed in Wimmer, 1994). The molecular mass of the MHC class I heavy chain (44 kDa) is compatible with that of plasma membrane protein species previously isolated by affinity chromatography on immobilized fiber or by cross-linking with adenovirions (Hennache and Boulanger, 1977; Svensson *et al.*, 1981; Belin and Boulanger, 1993). mAb 39B6, directed against human FNIII repeats 12–14, mAb B9.12.1 and mAb W6/32, the two latter directed against monomorphic determinants of the human class I MHC heavy chains, were tested individually in inhibition assays of Ad5Luc3 attachment to HeLa cells. A slight negative effect (2- to 2.5-fold) on luciferase gene expression was observed (not shown), suggesting that none of the mAb epitopes overlap the sequences which bind to the fiber knob.

The role of MHC-I α2 in Ad5/Ad2 cellular attachment did not preclude the occurrence of additional cell membrane protein ligands of Ad5 (or Ad2) fiber, acting as binding co-factors or auxiliary receptors with lower affinity constants, as already suggested (Haywood, 1994; Freimuth, 1996). This could be the case for FNIII modules, recognized in most eukaryotic tissues and prokaryotes (Bork and Doolittle, 1992), as well as for other virus receptors, such as the receptor of Coxsackie B3 (CB3), LDLR, the receptor of human rhinovirus 2 (HRV2), and ICAM-1, the receptor of HRV14 (Wimmer, 1994). CB3, HRV2 and HRV14 have been found to compete, partially or totally, with Ad2 for the same cell receptors (Lonberg-Holm *et al.*, 1976). Moreover, peptide ligands of Ad2

fiber have been identified as motifs present in ICAM-1 and LDLR (Hong and Boulanger, 1995). However, nothing is known about the functionality of these overlapping receptors with respect to the Ad life cycle, since competition with cold and labeled viruses has only been studied at the attachment level, and since 10–25% of cell-associated Ad has been found to be blocked at the stage of plasma membrane attachment (Belin and Boulanger, 1993; Wickham *et al.*, 1993). Further dissection of the mechanism of fiber–cell binding, and the nature of the protein partners involved at each discrete step will help the engineering of specifically cell-targeted adenoviral vectors (Michael *et al.*, 1995; Krasnykh *et al.*, 1996; Wickham *et al.*, 1996) used for gene therapy.

After completion of this work, we were informed of a study on the expression of Ad2 fiber receptors at the surface of mouse cells. Transfer of human chromosome 21 to the murine A9 cell line unable to bind Ad2 fiber conferred to cell transformants a fiber-mediated Ad2-binding capacity similar to that of human epithelial cells (Mayr and Freimuth, 1997). Since human class I MHC α chain is encoded by chromosome 6 and the β_2-microglobulin by chromosome 15, this would suggest that different plasma membrane components could serve as Ad2 and Ad5 fiber receptors in various cell contexts. Alternatively, human chromosome 21-encoded factor(s) could cooperate with or potentiate non-functional Ad2 fiber receptors in mouse cells. Interestingly, the gene coding for the integrin β_2-chain is located in chromosome 21 (Springer, 1990), and hematopoietic cells, which lack fiber-binding activity, use $\alpha_M\beta_2$ integrin as Ad2 receptor (Huang *et al.*, 1996).

Materials and methods

Mammalian cells and adenoviruses

HeLa cells were grown as monolayers in Dulbecco's modified Eagle's medium (Gibco) supplemented with 10% heat-inactivated fetal calf serum (FCS), L-glutamine and antibiotics. Daudi cells and β_2-microglobulin DNA-transformed Daudi cells (Daudi-HLA$^+$, E8.1 line; Quillet *et al.*, 1988) were maintained in RPMI 1640 (Gibco) supplemented with 15% FCS. Wild-type Ad5 and recombinant Ad5Luc3 were both propagated in HeLa cells. Ad5Luc3, obtained from F.Graham, is a replication-competent virus, which contains the luciferase gene under the control of the SV40 early promoter inserted in the E3 region of the Ad5 genome (Mittal *et al.*, 1993).

Insect cells and recombinant baculoviruses

The recombinant fiber knob domain and full-length fiber from three adenovirus serotypes, Ad2, Ad5 and Ad3, were expressed in *Spodoptera frugiperda* cells (Sf9), using recombinant *Autographa californica* nuclear polyhedrosis viruses (AcNPV). All our recombinant fiber proteins were expressed under the control of the polyhedrin promoter (Luckow and Summers, 1989), and the baculovirus intermediate transfer vector and cloning strategies have been described in detail previously (Novelli and Boulanger, 1991b; Karayan *et al.*, 1994).

The baculovirus clone expressing the Ad2 knob was obtained from J.Chroboczek (Louis *et al.*, 1994). It starts with a methionine residue at position 388, replacing an Ala residue in the wild-type Ad2 fiber sequence. To be consistent with our previous nomenclature (Novelli and Boulanger, 1991b), it was referred to as F2-AT388 in the present study, as it could be considered as an amino-truncated form of fiber reduced to its C-terminal knob and the last repeat unit of the shaft.

Likewise, F5-AT386 and F3-AT124 corresponded to Ad5 and Ad3 fiber knob domains, respectively, but also included the last shaft repeat. The last repeat has been found to be essential for stable trimerization of the knob domain (Henry *et al.*, 1994; Louis *et al.*, 1994). Both F5-AT386 and F3-AT124 were isolated by PCR amplification from Ad5 and Ad3 genomic DNAs, respectively, using the following pairs of primers. The forward 42mer oligonucleotide, from nucleotide 32 164 to 32 205 in the Ad5 genome (Chroboczek and Jacrot, 1987), 5′-CCT AAA CTA GGA TCC GGC CTT AGT TTT GAC AGC ATG GGT GCC-3′, included four mismatches (underlined) creating both a *Bam*HI site and an ATG initiator at position 388 in lieu of the Thr residue in wild-type Ad5 fiber. The reverse 37mer primer (32 919–32 883), 5′-CTG TGA GTT TGA TTA AGG TAC CGT GAT CTG TAT AAG C-3′, contained one single mismatch creating a *Kpn*I site. For F3-AT124, the forward 36mer primer (5′-GGT CTT ACA TTT GAC TCT TCC ATG GCT ATT GCA CTG-3′) introduced, via three mismatches generating a *Nco*I site, an ATG-specified initiation methionine in lieu of the Asn at position 124 (Signäs *et al.*, 1985), and an Ala in lieu of Ser125. The reverse 35mer primer, 5′-CAA TAA AAA ATG TGG TAC CTT ATT TTT GTT GTC AG-3′, contained a *Kpn*I site via three separate mismatches.

Baculovirus-expressed full-length Ad2 fiber (F2-FL582) has been described in previous studies (Novelli and Boulanger, 1991b). Recombinant full-length Ad5 fiber (F5-FL581) and full-length Ad3 fiber (F3-FL320) genes were generated by PCR amplification using Ad5 and Ad3 DNA as templates, and the above-described reverse primers for the Ad5 knob (37mer) and Ad3 knob (36mer), respectively. The 30mer forward primer 5′-CCA TCC GCA CCC ACT ATG ATC ACG TTG TTG-3′ (nucleotides 31 021–31 050) for Ad5 contained three mismatches, two generating a *Bgl*II-compatible *Bcl*I site, and one suppressing the in-phase upstream ATG. The 31mer forward primer 5′-CT TCA TTT CTT TAT CCC CCC ATG GCC A-3′ for Ad3 contained two mismatches generating an *Nco*I site.

The internal deletion (*dl*) mutant of Ad5 fiber, F5-*dl*314–402, was constructed like F5-FL581, from plasmid pTG8522, obtained from Transgene (Strasbourg). pTG8522 carried a deletion in the Ad5 fiber gene, from residue 314 to 402, corresponding to 89 amino acids from the shaft and the shaft–knob junction.

GST fusion peptides

The FNIII-derived pentadecapeptide RHILWTPANTPAMGY was added in fusion to the C-terminal end of the bacterially expressed GST. The oligonucleotide 5′-TC GAG AGG CAT ATA CTT TGG ACT CCT GCT AAT ACA CCG GCA ATG GGG TAT G-3′, and its complementary antisense oligonucleotide 5′-TC GAC ATA CCC CAT TGC CGG TGT ATT AGC AGG AGT CCA AAG TAT ATG CCT C-3′, were annealed and inserted into the unique *Xho*I site of the pGEX-KG plasmid (Guan and Dixon, 1991). The oligonucleotides were designed so as to regenerate the *Xho*I site at the 5′ end only if the insert was in the correct orientation. This allowed us to obtain sequentially longer constructs with single, tandem or multiple copies of the same insert in the restituted *Xho*I site. The final sequence of the C-terminus of the fusion protein containing one single insertion was GST-(thrombin-site)-PGIS-$(G)_5$-ILDSMGRLE-RHILWTPANTPAMGY(V)-E LKLNS-stop, and was referred to as GST–FN×1. Constructs with additional FN motifs (up to three) had each pentadecapeptide repeat inserted between residue L of the cloning cassette and residue E of the previous insert. They were referred to as GST–FN×2 and GST–FN×3, respectively. Similarly, the MHC-I α2-derived icosapeptide RAIVGFRVQWLRRYFVNGSR, was cloned at the GST C-terminus by insertion into the *Xho*I site of the following double-stranded oligonucleotide: 5′-TC GAG AGG GCT ATA GTT GGG TTT AGG GTG CAA TGG CTT AGG CGG TAT TTT GTG AAT GGG TCG AGG-3′ for the coding strand, and 5′-T CGA CCT CGA CCC ATT CAC AAA ATA CCG CCT AAG CCA TTG CAC CCT AAA CCC AAC TAT AGC CCT C-3′ for the antisense strand. As above, the icosapeptide repeats were inserted sequentially between residues LE and EL of the fusion cassette. The resulting fusion proteins were referred to as GST–MHC×1, GST–MHC×2 and GST–MHC×3.

Synthetic peptides

The two icosapeptides H_2N-RHILWTPANTPAMGYLARVS-CO_2H, referred to as FN20, and H_2N-RAIVGFRVQWLRRYFVNGSR-CO_2H, referred to as MH20, were synthesized and purified by Synt:em (Nîmes, France). As control unrelated peptides, lactalbumin enzymatic hydrolysate (Difco, tissue culture grade) was used at the same concentrations in virus-binding assays.

Fiber-binding assays

The GST fusion peptides, produced in bacterial cells, were extracted and purified by affinity on glutathione–agarose beads (Sigma) according to conventional methods (Smith and Johnson, 1988). The conditions used for *in vitro* binding of GST fusion peptides with recombinant fiber knob or full-length fiber, and recovering the protein complexes on glutathione–agarose beads, were those described by Johnson *et al.*

(1995). Fiber binding to synthetic peptides was assayed using a solid-phase method with MH20 and FN20 peptides immobilized on microtitration plates. The polystyrene surface of 96-well microtiter plates (Nunc Maxisorb) was coated overnight at 4°C with MH20 or FN20 at 5, 10 and 25 μM in phosphate-buffered saline (PBS). After rinsing and blocking with 3% bovine serum albumin in PBS, each well was reacted with increasing concentrations of radioactively labeled recombinant Ad5 fiber in PBS. Bound fiber was eluted with 1 M urea–1 M NaOH–1% SDS. Bound and unbound fiber were precipitated with 10% trichloroacetic acid (TCA), precipitates collected on a GF/C filter and counted in a liquid scintillation spectrometer (Beckman LS-6500). Baculovirus-expressed Fi5-FL581 was labeled with both [^{35}S]methionine and [^{35}S]cysteine as previously described (Hong and Boulanger, 1995). The specific radioactivity of the samples used was 50 000–65 000 c.p.m. per μg protein.

Electrophoresis and immunoblotting

SDS-denatured proteins were analyzed by SDS–PAGE in 12.5% acrylamide gels (acrylamide to bisacrylamide ratio of 50:0.8), using a discontinuous buffer system (Laemmli, 1970). Electric transfer of proteins onto nitrocellulose membranes (Hybond-ECL, Amersham) was carried out in 25 mM Tris–192 mM glycine buffer, pH 8.3, containing 20% methanol, at 0.8 mA/cm^2 for 90 min, using a semi-dry system (Cambridge Electrophoresis, Cambridge, UK). Blots were blocked with 5% skimmed milk and 1% calf serum in TBS-T buffer (20 mM Tris–HCl, pH 7.8, 0.15 M NaCl, 0.05% Tween-20), then successively reacted with primary antibody and horseradish peroxidase-labeled, anti-IgG conjugate. Immunological quantification of proteins was carried out as previously described (Chazal *et al.*, 1995), using chemiluminescent peroxidase substrate (SuperSignal, Pierce Chemicals). Luminograms (Hyperfilm-βmax, Amersham) were scanned at 610 nm, using an automatic densitometer system (REP-EDC, Helena Laboratories, Beaumont, TX).

Antibodies

Rabbit antisera against Ad2 virion proteins (Boudin and Boulanger, 1982), against electrophoretically purified recombinant Ad2 fiber protein (Novelli and Boulanger, 1991b) and recombinant GST were all laboratory made. mAb 4D2.5, directed against Ad fiber tail, was obtained from J.Engler (Hong and Engler, 1991). Mouse mAbs 1D6.3 and 7A2.7 were raised against bacterially expressed Ad5 fiber knob obtained from R.Gerard (Henry *et al.*, 1994), and were used as hybridoma cell culture supernatants (Michael *et al.*, 1993, 1995). Anti-FLAG M2 mAb (IBI) was used as control unrelated monoclonal antibody. Commercial mAbs against monomorphic epitopes of human class I HLA heavy chains were purchased from Immunotech (Marseille, France) for B9.12.1 (Malisen *et al.*, 1982), and from Dako (Glostrup, Denmark) for W6/32 (Barnstable *et al.*, 1978). mAb against anti-human fibronectin type III repeats 12–14 (clone 39B6) was obtained from Serotec (Oxford, UK).

Interference with Ad–cell attachment and virus neutralization

Five different assays were used.

Neutralization assay. The virus neutralization titer of mAbs 1D6.3 and 7A2.7 was determined by a conventional endpoint viral cytopathic effect (CPE) assay with crystal violet. In a standard procedure, wild-type Ad5 particles were incubated with hybridoma cell supernatant (undiluted to 1:128 dilution) in a total volume of 150 μl in culture medium for 30 min at room temperature, and the Ad–mAb mixture added to HeLa cell monolayers at 80% confluency (10^5 cells) at an m.o.i of 10 p.f.u./cell. Results were expressed as the maximum dilution which completely ablated adenoviral infection. Both 1D6.3 and 7A2.7 neutralized Ad5 at 1:64–1:128 dilution.

Cell attachment assay of Ad5. Aliquots of [methyl-^{3}H]thymidine-labeled wild-type Ad5 virions in PBS (specific radioactivity of 10^6 c.p.m. per 10^{11} virions) were added to HeLa cell monolayer samples at 10^5 c.p.m. per 10^5 cells, corresponding to 10^5 virions per cell, i.e. 10-fold the number of cell receptors (Persson *et al.*, 1985; Defer *et al.*, 1990; Seth *et al.*, 1994). Incubation proceeded for 1 h at 0°C, with or without mAb or peptide inhibitor, then the cells were rinsed, collected and dissolved in 1 M NaOH, 1% SDS, 1 M urea, and ^{3}H-labeled DNA was precipitated in 10% TCA on GF/C filters. TCA-precipitable radioactivity was counted in a liquid scintillation spectrometer (Beckman LS-6500).

Ad5–cell microbinding assay. mAb inhibition of Ad5–cell attachment was also assayed by using ^{14}C-labeled Ad5 virions and *in situ* cell autoradiography (Silver and Anderson, 1988). A constant input of [^{14}C]valine-labeled Ad5 with a specific radioactivity of 10^6 c.p.m. per 5×10^{10} virions was adsorbed on semiconfluent HeLa cell monolayers at an input of 10^3 virions per cell (corresponding to 10^3 c.p.m. per 5×10^4 cells) for 1 h at 0°C in the presence of mAbs at various concentrations. Cell samples were rinsed with PBS, fixed with 0.1% paraformaldehyde in PBS, dried and coated with Ilford nuclear research emulsion K4 in gel form. After a 1 week exposure at 4°C in light-proof boxes, the emulsion was developed using D19B developer (Kodak), and the specimens briefly colored with 0.5% toluidine blue in H_2O and examined under the light microscope. The density of reduced silver grains around the cell contour gave an estimation of the number of cell-bound ^{14}C-labeled Ad5 virions.

Ad5Luc3 attachment assay. Inhibition of Ad5–cell attachment was estimated from the level of luciferase gene expression, using the luciferase assay on Ad5Luc3-infected cells (Henry *et al.*, 1994). HeLa cells were infected with an increasing m.o.i. of Ad5Luc3, ranging from 0.02 to 0.2 f.f.u. per 10^5 cells, and luciferase activity (expressed in relative light units; RLU) was assayed in cell lysates at 18 h after infection, using luciferase substrate solution (Promega, Madison, WI). The reaction was carried out in a Lumat LB-9501 luminometer (Berthold Bioanalytical, Wildbad, Germany). Biological effects of synthetic peptides was determined in the linear range of dose–response, i.e. luciferase activity versus Ad5Luc3 m.o.i. Ad5Luc3 was pre-incubated with peptides at room temperature for 2 h, and the mixture added to HeLa cells pre-cooled on ice. After incubation for 1 h at 0°C, unadsorbed virus and peptide were rinsed off, the cell monolayers were covered with pre-warmed medium, transferred to 37°C and further incubated at this temperature for 18 h, then processed for luciferase assay.

Serotype specificity of Ad neutralization. The neutralization activity of synthetic peptides at the cell attachment step was assayed by immunotitration of the major Ad capsid proteins (Wohlfart, 1988). Ad5, Ad2 or Ad3 were pre-incubated with peptides at constant molarity (25 or 50 μM) and various m.o.i. (ranging from 0.2 to 5 f.f.u./cell) for 2 h at room temperature, and the mixture added onto HeLa cells at 0°C for 1 h. Then unadsorbed viruses were rinsed off and cells transferred to 37°C as described above. The level of synthesis of hexon, 100K protein, penton base and fiber was estimated using SDS–PAGE and immunoblot of cell extracts at 48 h after infection. Immunoblots were revealed by rabbit anti-Ad2 virion serum and peroxidase-labeled conjugate, and luminograms scanned as described above. Control experiments for possible cellular toxicity of peptides and cell viability in this and the previous assay consisted of pre-incubating HeLa cell monolayers with Ad for 1 h at 0°C, a temperature which only allows virus–cell attachment, or 37°C, a temperature at which both cell attachment and entry occur. Unadsorbed virus was then rinsed off and peptides added to the cells for 1 h at 37°C, at the post-attachment or post-entry steps.

Biopanning of the phage hexapeptide library on mAbs

The filamentous phage hexapeptide library was kindly provided by George Smith (fUSE5 phage; Scott and Smith, 1990). Affinity biopanning of phages to immobilized mAb was carried out following published protocols (Smith and Scott, 1993), with some modifications in terms of phage elution (Hong and Boulanger, 1995). In particular, to avoid the vast number of background sequences yielded by conventional acidic buffer elution, mAb-bound phages were selectively eluted using an excess of soluble recombinant Ad5 fiber knob (F5-AT386) as a competing ligand. The hexapeptide phagotopes were identified by DNA sequencing of the recombinant fUSE5 pIII protein, using the dideoxynucleotide chain termination method (Sanger *et al.*, 1977), oligonucleotide 5′-TGAATTTTCTGTATGAGG-3′ as the primer, and Sequenase kit version 2.0 (USB-Sequenase, Amersham). The search for sequence homology was performed using the SwissProt protein database and the FASTA 1.6 program (Pearson and Lipman, 1988). Multiple sequence alignment was performed using the W(1.4) version of the Clustal program (Higgins and Sharp, 1988).

Acknowledgements

We thank Arnaud Dupuy d'Angeac for fruitful discussions and help in flow cytometry analysis, and Bernard Gay for iconography. We are grateful to Jeff Engler and Jeong-Shin Hong for their gift of mAb 4D2.5, Frank Graham for Ad5Luc3, Christian Devaux for Daudi cells, Didier Fradelizi for the Daudi-HLA$^+$ E8.1 cell line, Jadwiga Chroboczek for recombinant baculovirus expressing the Ad2 knob, George Santis and Valérie Legrand for plasmid pTG8522 and Sharon Michael for CPE neutralization assays with mAbs 1D6.3 and 7A2.7. This work was

supported in part by the Association Française de Lutte contre la Mucoviscidose and the Association Française contre les Myopathies (AFLM grant 96022), and Transgene SA (Strasbourg). S.S.H. was the recipient of a fellowship from the AFLM. D.T.C. was supported by the grants NIH-RO1 5025505 and US Army-DAMD 17-94-J-4398, and the Muscular Dystrophy Association.

References

Bai,M., Harfe,B. and Freimuth,P. (1993) Mutations that alter an Arg–Gly–Asp (RGD) sequence in the adenovirus type 2 penton base protein abolish its cell-rounding activity and delay virus reproduction in flat cells. *J. Virol.*, **67**, 5198–5205.

Bai,M., Campisi,L. and Freimuth,P. (1994) Vitronectin receptor antibodies inhibit infection of HeLa and A549 cells by adenovirus type 12 but not by adenovirus type 2. *J. Virol.*, **68**, 5925–5932.

Barnstable,C.J., Bodmer,W.F., Brown,G., Galfre,G., Milstein,C., Williams,A.F. and Ziegler,A. (1978) Production of monoclonal antibodies to group A erythrocytes, HLA and other human cell surface antigens—new tools for genetic analysis. *Cell*, **14**, 9–20.

Belin,M.T. and Boulanger,P. (1993) Involvement of cellular adhesion sequences in the attachment of adenovirus to the HeLa cell surface. *J. Gen. Virol.*, **74**, 1485–1497.

Bjorkman,P.J. and Parham,P. (1990) Structure, function, and diversity of class I major histocompatibility complex molecules. *Annu. Rev. Biochem.*, **59**, 253–288.

Bork,P. and Doolittle,R.F. (1992) Proposed acquisition of an animal protein domain by bacteria. *Proc. Natl Acad. Sci. USA*, **89**, 8990–8994.

Boudin,M.-L. and Boulanger,P. (1982) Assembly of adenovirus penton base and fiber. *Virology*, **116**, 589–604.

Breau,W.C., Atwood,W.J., and Norkin,L.C. (1992) Class I major histocompatibility proteins are an essential component of the simian virus 40 receptor. *J. Virol.*, **66**, 2037–2045.

Chazal,N., Gay,B., Carrière,C., Tournier,J. and Boulanger,P. (1995) Human immunodeficiency virus type 1 MA deletion mutants expressed in baculovirus-infected cells: *cis* and *trans* effects on the Gag precursor assembly pathway. *J. Virol.*, **69**, 365–375.

Chroboczek,J., Ruigrok,R.W.H. and Cusack,S. (1995) Adenovirus fiber. *Curr. Top. Microbiol. Immunol.*, **199**, 163–200.

Cuzange,A., Chroboczek,J. and Jacrot,B. (1994) The penton base of human adenovirus type 3 has the RGD motif. *Gene*, **146**, 257–259.

Defer,C., Belin,M.T., Caillet-Boudin,M.L. and Boulanger,P. (1990) Human adenovirus–host cell interactions: a comparative study with members of subgroups B and C. *J. Virol.*, **64**, 3661–3673.

Dickinson,C.D., Veerapandian,B., Dai,X.-P., Hamlin,R.C., Xuong,N.-H., Ruoslahti,E. and Ely,K.R. (1994) Crystal structure of the tenth type III cell adhesion module of human fibronectin. *J. Mol. Biol.*, **236**, 1079–1092.

Fender,P., Kidd,A.H., Brebant,R., Öberg,M., Drouet,E. and Chroboczek,J. (1995) Antigenic sites on the receptor-binding domain of human adenovirus type 2 fiber. *Virology*, **214**, 110–117.

Freimuth,P. (1996) A human cell line selected for resistance to adenovirus infection has reduced levels of the virus receptor. *J. Virol.*, **70**, 4081–4085.

Goldman,M.J. and Wilson,J.M. (1995) Expression of $\alpha_V\beta_5$ integrin is necessary for efficient adenovirus-mediated gene transfer in the human airway. *J. Virol.*, **69**, 5951–5958.

Greber,U.F. and Kasamatsu,H. (1996) Nuclear targeting of SV40 and adenovirus. *Trends Cell Biol.*, **6**, 189–195.

Greber,U.F., Willetts,M., Webster,P. and Helenius,A. (1993) Stepwise dismantling of adenovirus 2 entry into cells. *Cell*, **75**, 477–486.

Guan,K.L. and Dixon,J.E. (1991) Eukaryotic proteins expressed in *Escherichia coli*: an improved thrombin cleavage and purification procedure of fusion proteins with glutathione *S*-transferase. *Anal. Biochem.*, **192**, 262–267.

Haywood,A.M. (1994) Virus receptors: adhesion, strengthening, and changes in viral structure. *J. Virol.*, **68**, 1–5.

Hennache,B. and Boulanger,P.A. (1977) Biochemical study of KB cell receptor for adenovirus. *Biochem. J.*, **166**, 237–247.

Henry,L., Xia,D., Wilke,M., Deisenhofer,J. and Gerard,R.D. (1994) Characterization of the knob domain of the adenovirus type 5 fiber protein expressed in *E.coli*. *J. Virol.*, **68**, 5239–5246.

Higgins,D.G. and Sharp,P.M. (1988) Clustal: a package for performing multiple sequence alignment on a microcomputer. *Gene*, **73**, 237–244.

Hong,S.S. and Boulanger,P. (1995) Protein ligands of the human adenovirus type 2 outer capsid identified by biopanning of a phage-displayed peptide library on separate domains of wild-type and mutant penton capsomers. *EMBO J.*, **14**, 4714–4727.

Hong,J.S. and Engler,J.A. (1991) The amino terminus of the adenovirus fiber protein encodes the nuclear localization signal. *Virology*, **185**, 758–767.

Hong,J.S. and Engler,J.A. (1996) Domains required for assembly of adenovirus type 2 fiber trimers. *J. Virol.*, **70**, 7071–7078.

Huang,S., Kamata,T., Takada,Y., Ruggeri,Z.M. and Nemerow,G.R. (1996) Adenovirus interaction with distinct integrins mediates separate events in cell entry and gene delivery to hematopoietic cells. *J. Virol.*, **70**, 4502–4508.

Johnson,E.M., Chen,P.-L., Krachmarov,C.P., Barr,S.H., Kanovski,M., Ma,Z.-W. and Lee,W.-H. (1995) Association of human Purα with the retinoblastoma protein, Rb, regulates binding to the single-stranded DNA Purα recognition element. *J. Biol. Chem.*, **270**, 24352–24360.

Karayan,L., Gay,B., Gerfaux,J. and Boulanger,P. (1994) Oligomerization of recombinant penton base of adenovirus type 2 and its assembly with fiber in baculovirus-infected cells. *Virology*, **202**, 782–796

Krasnykh,V.N., Mikheeva,G.V., Douglas,J.T. and Curiel,D.T. (1996) Generation of recombinant adenovirus vectors with modified fibers for altering viral tropism. *J. Virol.*, **70**, 6839–6846.

Laemmli,U.K. (1970) Cleavage of structural proteins during assembly of the head of bacteriophage T4. *Nature*, **227**, 680–685.

Lonberg-Holm,K. and Philipson,L. (1969) Early events of virus-cell interaction in an adenovirus system. *J. Virol.*, **4**, 323–338.

Lonberg-Holm,K., Crowell,R.L. and Philipson,L. (1976) Unrelated animal viruses share receptors. *Nature*, **259**, 679–681.

Louis,N., Fender,P., Barge,A., Kitts,P. and Chroboczek,J. (1994) Cell-binding domain of adenovirus serotype 2 fiber. *J. Virol.*, **68**, 4104–4106.

Luckow,V.A. and Summers,M.D. (1989) High level expression of nonfused foreign genes with *Autographa californica* nuclear polyhedrosis virus expression vectors. *Virology*, **170**, 31–39.

Main,A.L., Harvey,T.S., Baron,M., Boyd,J. and Campbell,I.D. (1992) The three-dimensional structure of the tenth type III module of fibronectin: an insight into RGD-mediated interactions. *Cell*, **71**, 671–678.

Malisen,B., Rebai,N., Liabeuf,A. and Mawas,C. (1982) Human cytotoxic T cell structures associated with expression of cytolysis. I. Analysis at the clonal cell level of the cytolysis-inhibiting effect of 7 monoclonal antibodies. *Eur. J. Biochem.*, **12**, 739–747.

Masse,R. (1976) Action of radiations on nuclear emulsions. *J. Microsc. Biol. Cell.*, **27**, 83–90.

Mathias,P., Wickham,T., Moore,M. and Nemerow,G. (1994) Multiple adenovirus serotypes use α_V integrins for infection. *J. Virol.*, **68**, 6811–6814.

Mayr,G.A. and Freimuth,P. (1997) A single locus on human chromosome 21 directs the expression of a receptor for adenovirus type 2 in mouse A9 cells. *J. Virol.*, **71**, 412–418.

Messer,G., Zemmour,J., Orr,H.T., Parham,P., Weiss,E.H. and Girdlestone,J. (1992) HLA-J, a second inactivated class I HLA gene related to HLA-G and HLA-A. Implications for the evolution of the HLA-A-related genes. *J. Immunol.*, **148**, 4043–4053.

Michael,S.I., Huang,C.H., Romer,M.U., Wagner,E., Hu,P.C. and Curiel,D.T. (1993) Binding-incompetent adenovirus facilitates molecular conjugate-mediated gene transfer by the receptor-mediated endocytosis pathway. *J. Biol. Chem.*, **268**, 6866–6869.

Michael,S.I., Hong,J.S., Curiel,D.T. and Engler,J.A. (1995) Addition of a short peptide ligand to the adenovirus fiber protein. *Gene Ther.*, **2**, 660–668.

Mittal,S.K., McDermott,M.R., Johnson,D.C., Prevec,L. and Graham,F.L. (1993) Monitoring foreign gene expression by a human adenovirus-based vector using the firefly luciferase gene as a reporter. *Virus Res.*, **28**, 67–90.

Nemerow,G.R., Cheresh,D.A. and Wickham,T.J. (1994) Adenovirus entry into host cells: a role for αv integrins. *Trends Cell Biol.*, **4**, 52–55.

Novelli,A. and Boulanger,P. (1991a) Assembly of adenovirus type 2 fiber synthesized in cell-free translation system. *J. Biol. Chem.*, **266**, 9299–9303.

Novelli,A. and Boulanger,P. (1991b) Deletion analysis of functional domains in baculovirus-expressed adenovirus type 2 fiber. *Virology*, **185**, 365–376.

Pearson,W.R. and Lipman,D.J. (1988) Improved tools for biological sequence comparison. *Proc. Natl Acad. Sci. USA*, **85**, 2444–2448.

Persson,R., Svensson,U. and Everitt,E. (1985) Virus–receptor interaction in the adenovirus system: characterization of the positive cooperative binding of virions on HeLa cells. *J. Virol.*, **54**, 92–97.

Philipson,L., Lonberg-Holm,K. and Pettersson,U. (1968) Virus–receptor interaction in an adenovirus system. *J. Virol.*, **2**, 1064–1075.
Quillet,A., Presse,F., Marchiol-Fournigault,C., Harel-Bellan,A., Benbunan,M., Ploegh,H. and Fradelizi,D. (1988) Increased resistance to non-MHC-restricted cytotoxicity related to HLA A, B expression: direct demonstration using β2-microglobulin-transfected Daudi cells. *J. Immunol.*, **141**, 17–20.
Sanger,F., Nicklen,S. and Coulson,A.R. (1977) DNA sequencing with chain terminating inhibitors. *Proc. Natl Acad. Sci. USA*, **74**, 5463–5467.
Scatchard,G. (1949) The attraction of proteins for small molecules and ions. *Ann. N.Y. Acad. Sciences*, **51**, 660–672.
Scott,J.K. and Smith,G.P. (1990) Searching for peptide ligands with an epitope library. *Science*, **249**, 386–390.
Seth,P., Rosenfeld,M., Higginbotham,J. and Crystal,R.G. (1994) Mechanism of enhancement of DNA expression consequent to cointernalization of a replication-deficient adenovirus and unmodified plasmid DNA. *J. Virol.*, **68**, 933–940.
Silver,L. and Anderson,C.W. (1988) Interaction of human adenovirus serotype 2 with human lymphoid cells. *Virology*, **165**, 377–387.
Smith,D.B. and Johnson,K.S. (1988) Single-step purification of polypeptides expressed in *Escherichia coli* as fusions with glutathione *S*-transferase. *Gene*, **67**, 31–40.
Smith,G.P. and Scott,J.K. (1993) Libraries of peptides and proteins displayed on filamentous phage. *Methods Enzymol.*, **217**, 228–257.
Sprengel,J., Schmitz,B., Heuss-Neitzel,D., Zock,C. and Doerfler,W. (1994) Nucleotide sequence of human adenovirus type 12 DNA: comparative functional analysis. *J. Virol.*, **68**, 379–389.
Springer,T.A. (1990) Adhesion receptors of the immune system. *Nature*, **346**, 425–434.
Stevenson,S.C., Rollence,M., White,B., Weaver,L. and McClelland,A. (1995) Human adenovirus serotypes 3 and 5 bind to two different cellular receptors via the fiber head domain. *J. Virol.*, **69**, 2850–2857.
Svensson,U. (1985) Role of vesicles during adenovirus 2 internalization into HeLa cells. *J. Virol.*, **55**, 442–449.
Svensson,U. and Persson,R. (1984) Entry of adenovirus 2 into HeLa cells. *J. Virol.*, **51**, 687–694.
Svensson,U., Persson,R. and Everitt,E. (1981) Virus–receptor interactions in the adenovirus system. I. Identification of virion attachment proteins of the HeLa cell plasma membrane. *J. Virol.*, **38**, 70–81.
Varga,M., Weibull,C. and Everitt,E. (1991) Infectious entry pathway of adenovirus type 2. *J. Virol.*, **65**, 6061–6070.
Watson,G., Burdon,M.G. and Russell,W.C. (1988) An antigenic analysis of the adenovirus type 2 fibre polypeptide. *J. Gen. Virol.*, **69**, 525–535.
White,J.M. (1993) Integrins as virus receptors. *Curr. Biol.*, **3**, 596–599.
Wickham,T.J., Mathias,P., Cheresh,D.A. and Nemerow,G.R. (1993) Integrins $\alpha_v\beta_3$ and $\alpha_v\beta_5$ promote adenovirus internalization but not virus attachment. *Cell*, **73**, 309–319.
Wickham,T.J., Filardo,E.J., Cheresh,D.A. and Nemerow,G.R. (1994) Integrin $\alpha_v\beta_5$ selectively promotes adenovirus mediated cell membrane permeabilization. *J. Cell Biol.*, **127**, 257–264.
Wickham,T.J., Segal,D.M., Roelvink,P.W., Carrion,M.E., Lizonova,A., Lee,G.M. and Kovesdi,I. (1996) Targeted adenovirus gene transfer to endothelial and smooth muscle cells by using bispecific antibodies. *J. Virol.*, **70**, 6831–6838.
Wimmer,E. (1994) Introduction. In Wimmer,E. (ed.), *Cellular Receptors for Animal Viruses*. Cold Spring Harbor Laboratory Press, Cold Spring Harbor, NY, pp. 1–13.
Wohlfart,C. (1988) Neutralization of adenoviruses: kinetics, stoichiometry, and mechanisms. *J. Virol.*, **62**, 2321–2328.
Xia,D., Henry,L.J., Gerard,R.D. and Deisenhofer,J. (1994) Crystal structure of the receptor-binding domain of adenovirus type 5 fiber protein at 1.7 Å resolution. *Curr. Biol. Struct.*, **2**, 1259–1270.

Received on November 18, 1996; revised on January 21, 1997